Volume 1 | Number 1 | Jan 2013 | Pages 1–100

Catalysis
Science &
Technology

www.rsc.org/catalysis

ROYAL SOCIETY
OF CHEMISTRY

ROYAL SOCIETY
OF CHEMISTRY

www.rsc.org/catalysis

1   A Density Functional Theory Study on Ethylene Formation and Conversion over P

2   Modified ZSM-5

3   Yanping Huang, Xiuqin Dong, Mengmeng Li, Yingzhe Yu *

4   Key Laboratory for Green Chemical Technology of Ministry of Education,

5   R&D Center for Petrochemical Technology, Tianjin University

6   Tianjin 300072, P R China

7   * Corresponding author. Tel.: +86-22-27405972; fax: +86-22-27406119.

8   E-mail address: yzhyu@tju.edu.cn (Yingzhe Yu)

9

10   **Abstract:** In this work, Density Functional Theory (DFT) was used to choose the

11   suitable ZSM-5 model. The effect of P modification of ZSM-5 on the rate-limiting

12   step of stepwise reaction pathway of ethylene dimerization, that is, ethylene

13   protonation, was studied. 14T was used to search the transition state. On the

14   extra-framework modified H_3PO_4/HZSM-5 zeolite, the adsorption energy of ethylene

15   decreases, which makes the products desorb quickly after formation and reduces the

16   incidence of dimerization or polymerization. Ethylene polymerization reaction is the

17   main cause of coking deactivation of ZSM-5. That ethylene protonation reaction is the

18   rate-limiting step of ethylene dimerization suggests that after P modification, the

19   activation energy of ethylene dimerization increases to inhibit ethylene dimerization,

20   prevent deep ethylene polymerization and thus improve the resistance to coke

21   deposition of ZSM-5 and prolong the life of zeolite. Based on the study results, the

22   inhibition mechanism of P modification to ethylene dimerization was explored to

1 provide beneficial theoretical guide for designing and improving the catalyst of

2 ethanol dehydration to ethylene.

3 **Keywords:** Density Functional Theory (DFT); Ethylene Dimerization; Phosphorus

4 acid; ZSM-5 zeolite

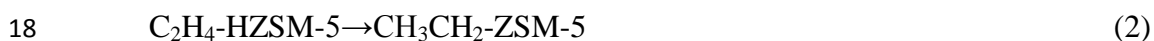5 **1. Introduction**

6   The development level of ethylene industry is one of the important indicators to

7 measure the economic power of a country. And it plays an important role in the

8 national economy development. Global oil resources are becoming increasingly

9 strained, thus severely restricting the development of ethylene industry. The

10 exploitation of various non-oil raw materials for ethylene production is drawing the

11 worldwide attention. Ethanol dehydration to ethylene has broad development

12 prospects, and plays an important role in promoting the economic development and

13 environmental protection [1, 2, 3, 4].

14   Over 200 years ago, Bondt et al. was first to detect the selective conversion of

15 ethanol to ethylene in mildly acidic homogeneous solution[5]. Activated alumina

16 (γ-A1$_2$O$_3$) shows relatively high activity and selectivity, when used as the catalyst of

17 ethanol dehydration reaction. At present, the catalyst employed in industry is mainly

18 γ-A1$_2$O$_3$. However, when γ-A1$_2$O$_3$ is used as the catalyst, some problems exist. For

19 example, the concentration of the reactant ethanol is required to be relatively high,

20 which is usually higher than 95% (volume fraction); the production capacity of

21 operation equipment is relatively small, and the energy consumption is relatively large;

22 the reaction temperature is relatively high, which is usually about 380℃[6]. Since

1   1980s, researchers have been using zeolite to catalyze ethanol dehydration to ethylene

2   reaction. The zeolites used mainly include H-NaZSM-5 zeolite, HZSM-5 with various

3   ratios of silica to alumina, SAPO-34 zeolite, HBeta zeolite, 4A zeolite, H- mordenite,

4   V-MCM-41, HY zeolite and so on[7, 8, 9, 10]. Among those zeolites, ZSM-5 is often

5   used in the catalytic dehydration study because of its relatively good lipophilic and

6   hydropholic property. When ZSM-5 is used in ethanol dehydration to ethylene

7   reaction, under the condition of the temperature of 250~300℃ and space velocity of

8   1~2h^{-1}, the conversion is above 99.5% and the selectivity is above 99.4%[11].

9   Phillips et al. studied the dehydration reaction over HZSM-5 of ethanol solution

10 with various volume concentrations (80~100%)[5]. They found that coke deposition is

11 significant for HZSM-5. In order to improve aforementioned problems, researchers

12 modified ZSM-5 through such methods as hydrothermal treatment, ion exchange and

13 impregnation [12, 13, 14, 15]. Murata et al.[16] studied the influence of P content of

14 P-ZSM-5 on modification effect. They found that with P content of P-ZSM-5

15 increasing, conversion of ethanol increases and the selectivity of ethylene increases

16 significantly. However, excess p destroys the Bronsted acid sites on the surface of

17 ZSM-5. The researches of Zhang et al.[17] showed that when P content of P-ZSM-5 is

18 3.4wt%(P/Al=0.95), the main product of ethanol dehydration reaction is ethylene,

19 with the selectivity of ethylene larger than 99.4%, and the reaction temperature

20 ranging from 573K to 713K. Ramesh et al.[18] prepared a series of P-ZSM-5 with

21 various P content and applied them in the ethanol dehydration to ethylene reaction.

22 They found that the introduction of P into ZSM-5 will reduce the adsorption of

polymer in reaction and thus improve the selectivity and thermostability of the catalyst. C_5^+, especially aromatic hydrocarbons, obviously exist on the catalyst after reaction, resulting in coke deposition in the ZSM-5 without P, while in P modified ZSM-5, the catalyst is still active after the reaction undergoes 200h, suggesting the lifetime of P modified ZSM-5 increases. That is to say, under these conditions, the ethylene dimerization reaction may lead to coke deposition which will cause the catalyst to be deactivated[19,20]. Due to the pore confinement effect, ZSM-5 zeolites are effective catalysts for ethylene dimerization[21]. Currently, many researchers base their studies of ethylene dimerization on the stepwise and concerted mechanisms[21, 22, 23, 24, 25]. Zhang Jia et al. conducted a theoretical study on the stepwise pathway of dimerization reaction and concerted dimerization reaction pathway of ethylene on HZSM-5[26]. The calculation results showed that concerted reaction needs more activation energy, and thus the dimerization reaction of ethylene on HZSM-5 occurs as the stepwise reaction, in which the first step that the ethylene molecule is protonated is the rate-limiting step. The stepwise reaction pathway is shown as follows:

$$C_2H_4 + HZSM\text{-}5 \rightarrow C_2H_4\text{-}HZSM\text{-}5 \tag{1}$$

$$C_2H_4\text{-}HZSM\text{-}5 \rightarrow CH_3CH_2\text{-}ZSM\text{-}5 \tag{2}$$

$$CH_3CH_2\text{-}ZSM\text{-}5 + C_2H_4 \rightarrow C_4H_9\text{-}ZSM\text{-}5 \tag{3}$$

In this work, Density Functional Theory (DFT) was used to choose the suitable ZSM-5 model. The effect of P modification of ZSM-5 on the rate-limiting step of stepwise reaction pathway of ethylene dimerization, that is, ethylene protonation, was

1   studied. This study was conducted to explore the effect of P modification on ethylene

2   dimerization. Based on the study results, the inhibition mechanism of P modification

3   to ethylene dimerization was explored to provide beneficial theoretical guide for

4   designing and improving the catalyst of ethanol dehydration to ethylene to reduce

5   coke deposition which will deactivate the catalyst.

6   **2.   Computational Model and Methods**

7   ZSM-5 zeolite has the MFI framework topology, characterized by a

8   three-dimensional pore system with straight and sinusoidal channels. The pore

9   vacancies are defined by 10 member oxygen-rings that are wide enough (about 5.5 Å)

10   to allow molecules as large as benzene to pass. As is shown in Figure 1, among the

11   twelve crystallographic distinct T sites, T4 and T10 sites, marked in green, only

12   appear in the 10 member O-ring which forms the straight channel. Similarly, T8 and

13   T11 sites, marked in blue, only appear in the 10 member O-ring which forms the

14   sinusoidal channel. Thus, there are eight T sites which are common to both straight

15   and sinusoidal channels [27, 28]. Many studies reported that the T6, T9 and T12 sites,

16   marked in purple, are the most stable positions for Al atoms [29,30,31], but some

17   other studies suggested that T12 site is the most stable position for Al atoms [32, 33,
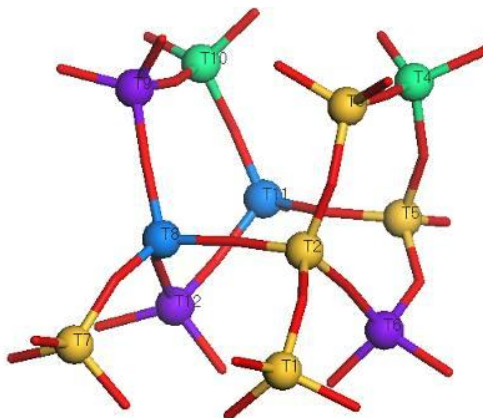
18   34, 35, 36].

19

1

Figure 1 The unit structure of ZSM-5 zeolite

3   To avoid the influence of the size of the cluster model, the 8T, 14T and 18T

4   models of ZSM-5 are respectively optimized and compared to choose the most

5   suitable size of cluster model. Only the situation that the T12 site is replaced by Al is

6   taken into consideration in this study.

7   All calculations were performed using DMol^3 module of MS (Materials Studio)

8   [37, 38]. In the DFT simulation, the generalized gradient approximation (GGA) in the

9   RPBE parameterization was used in all calculations. With the consideration of the

10   electronic polarization effect, the double numerical plus polarization (DNP) basis set

11   was used in the calculation. The numerical basis sets in DMol3 minimize or even

12   eliminate basis set superposition error (BSSE) in contrast to Gaussian basis sets,

13   where BSSE can be a serious problem[39, 40]. The transition state was completely

14   determined by LST/QST. The allowable deviations of the total energy, gradient and

15   displacement are 1×10^{-5}Ha, 0.004Ha/Å and 0.005Å, respectively.

16   **3.   Results and Discussion**

17   **3.1 The Comparison of 8T, 14T and 18T**

18   **3.1.1 Unmodified HZSM-5**

1 The acidity of zeolite plays an important role in the ethanol dehydration reaction.

2 Acidic properties can influence the reaction activity of zeolites as acid catalysts, and

3 the acid strength can be influenced by the chemical composition, such as the

4 species[41]. Studies suggest that the deprotonation energy (DPE) is an effective way

5 to measure the acidity of zeolite. Deprotonation energy cannot be directly measured

6 experimentally. Deprotonation energy denotes the energy that it takes to remove an

7 acidic proton from the zeolite. It can be shown in the following Formula (1),

8 $Zeo\text{-}OH \rightarrow Zeo\text{-}O^- + H^+$ Formula (1)

9 The deprotonation energy (*DPE*) of zeolite, $DPE = E_{Zeo\text{-}OH} - E_{Zeo\text{-}O^-}$, where $E_{Zeo\text{-}OH}$

10 and $E_{Zeo\text{-}O^-}$ represent the energy of zeolite before and after the removal of proton. The

11 smaller the *DPE* is, the easier it is to remove the proton, and the stronger the acidity

12 of zeolite is.

13 Figure 2 shows the optimized configurations of 8T, 14T and 18T when HZSM-5

14 is not modified. The specific parameters and the deprotonation energy can be seen in

15 Table 1. The 8T model is 1/3 of the entire channel. The 14T model is 1/2 of the entire

16 channel. The 18T model is the whole channel. Table 1 shows that the numbers of

17 atoms contained in each model are 34, 58 and 73, respectively. The number of atoms

18 contained in the 18T model is more than double of the number of atoms contained in

19 the 8T model. In the quantum chemical calculations, the larger the number of atoms

20 contained in the model is, the slower the computation is. Thus, to save some

21 computational time and ensure that the computation model is as close to the reaction

1   system as possible, with the premise that it is ensured that the model parameters are

2   not influenced by the model size, relatively small model should be adopted.

3   From Figure 2, the bond lengths of bridge hydroxyls in 8T, 14T and 18T models

4   are 0.975Å, 0.975Å, 0.976Å, respectively, which are almost equivalent and all are

5   consistent with the calculation value of Xin[42]. The deprotonation energies of those

6   models are 298.18kcal/mol, 295.22kcal/mol and 295.72kcal/mol, respectively, which

7   are all in the experimental value range of 291~300kcal/mol[43] and are in good

8   agreement with the study result of Brandle, 1200 kJ/mol (286.68kcal/mol) [44] , and

9   the study result of Zheng, 294 kcal/mol[45].
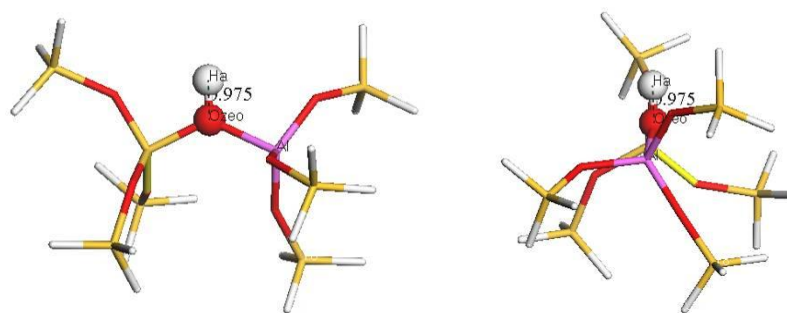
10

11   (a) 8T

12

13   (b) 14T

14
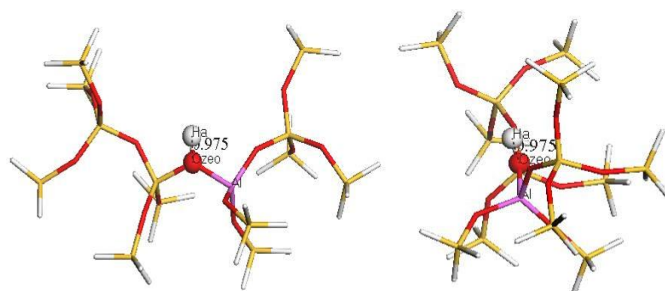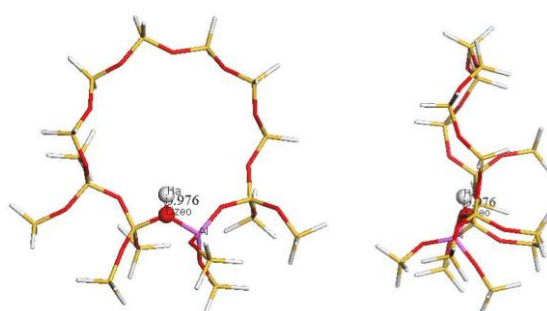
1 (c) 18T

2 Figure 2 The configurations of unmodified ZSM-5 zeolite cluster models

3 Table 1 The deprotonation energy of the unmodified ZSM-5 zeolite cluster models

Model	atoms	O_{zeo}-H_a (Å)	E_{Zeo-OH} (Ha)	E_{Zeo-O-} (Ha)	DPE (kcal/mol)
8T	34	0.975	-2807.7426	-2807.2675	298.18
14T	58	0.975	-5004.0379	-5003.5675	295.22
18T	73	0.976	-6542.4003	-6541.9290	295.72
Experiment	-	-	-	-	291~300[43]

4 Besides the comparison of the geometry structure of each model, in this study,

5 adsorption energy of ethanol was also compared. In the Figure 3, the stable

6 configurations of ethanol molecules adsorbed on unmodified 8T, 14T and 18T models

7 are shown. Table 2 lists the geometric parameters and adsorption data of the ethanol

8 adsorption on each model. The adsorption energy of ethanol can be shown in the

9 following Formula (2):

10 $E_a=E_{T-C2H5OH}-E_T-E_{C2H5OH}$ Formula (2)

11 Where, E_a represents the adsorption energy of ethanol, *kcal/mol;*

12 $E_{T-C2H5OH}$ represents the total energy of the system after ethanol is adsorbed on

13 the catalyst surface, *Ha;*

14 E_T represents the total energy before adsorption, *Ha;*

15 E_{C2H5OH} represents the total energy of ethanol before adsorption, *Ha;*

16 1Ha=627.51kcal/mol.

1

2   (a) 8T

3

4   (b) 14T

5

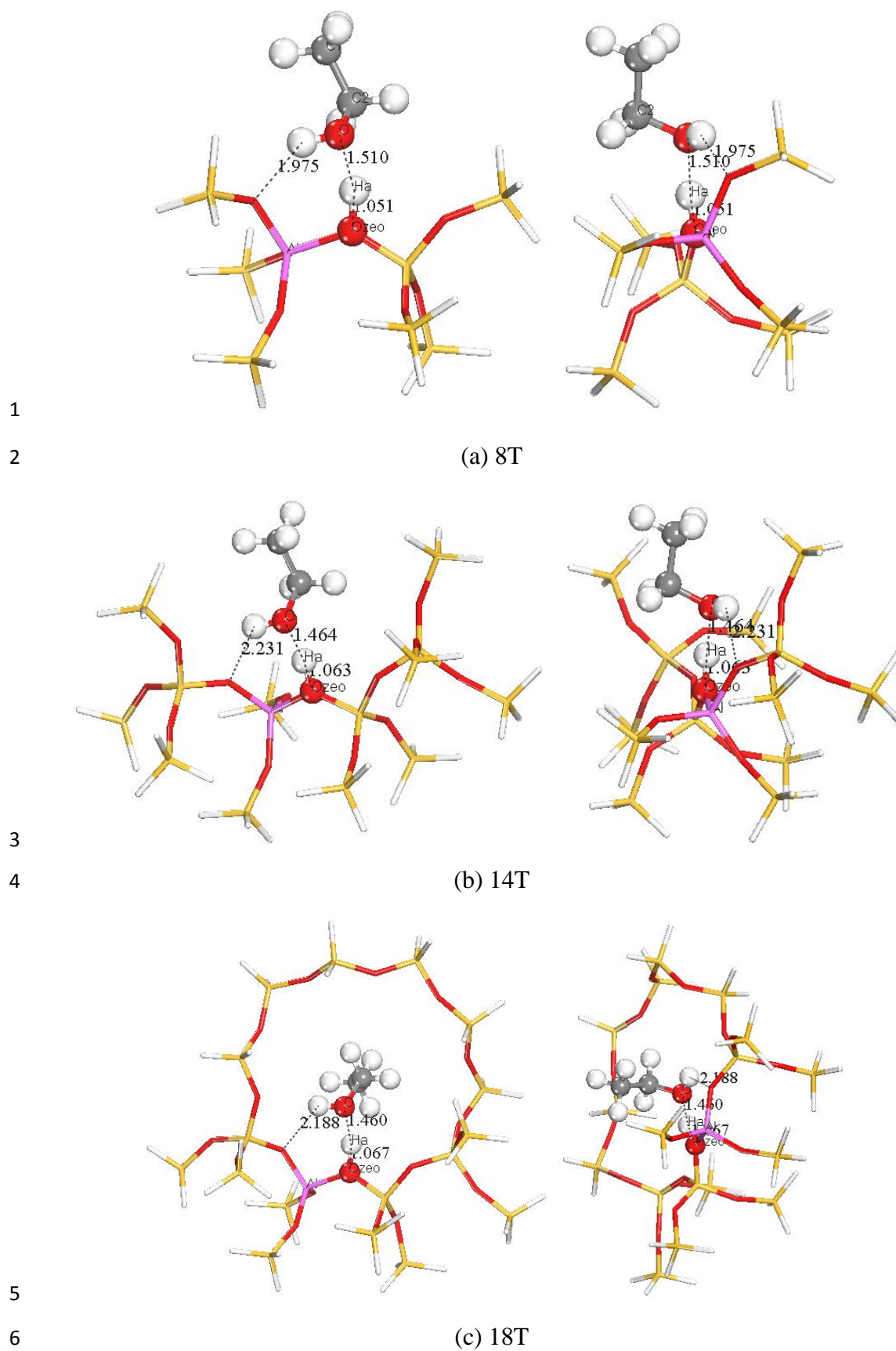6   (c) 18T

7   Figure 3 The optimized models of ethanol absorbed on unmodified ZSM-5 zeolite

1   Table 2 Adsorption energy of the ethanol adsorbed on unmodified ZSM-5 zeolite

| Model	O_{zeo}-H_a (Å)	O-H_a (Å)	E_T (Ha)	E_{C2H5OH} (Ha)	$E_{T\text{-}C2H5OH}$ (Ha)	E_a (kcal/mol)
8T	1.051	1.510	-2807.7426	-155.0447	-2962.8152	-17.50
14T	1.063	1.464	-5004.0379	-155.0447	-5159.1118	-18.32
18T	1.067	1.460	-6542.4003	-155.0447	-6697.4744	-18.50

2

3   From Figure 3, the O atom of ethanol is adsorbed on the H atom of bridge

4   hydroxyl of the zeolite in the 8T, 14T and 18T models. The H atom of hydroxyl in

5   ethanol molecule always prefers the Al atom in the zeolite. The three models show

6   almost no difference from the perspective of the adsorption configuration. From the

7   adsorption data listed in Figure 3, the distances between the O atom of ethanol

8   molecules and H atoms of bridge hydroxyl of zeolite are 1.510Å, 1.464Å and 1.460Å,

9   respectively. The bond lengths of bridge hydroxyl of zeolite are 1.051Å, 1.063Å and

10   1.067Å, with the difference between each other within 0.1Å, suggesting the O atom of

11   ethanol molecule forms hydrogen bond with the bridge hydroxyl of the zeolite. The

12   adsorption energy of each configuration is -17.50kcal/mol, -18.32kcal/mol and

13   -18.50kcal/mol, respectively, with the difference within 1kcal/mol, suggesting the

14   difference of adsorption energy data of ethanol adsorption on each model is not

15   significant. And all the values are close to the experimental values of Lee, -130±5

16   kJ/mol (31.05±1.20 kcal/mol)[46].

17   In the summary, as for unmodified HZSM-5, the results of geometric parameters

1   and deprotonation energy of each model are almost the same, whether it is the

2   optimized zeolite model or the zeolite configuration with ethanol adsorbed. Thus, 8T,

3   14T and 18T all can be used to study the related properties of unmodified HZSM-5.

4   **3.1.2 Extra-framework Modified H₃PO₄/HZSM-5 Zeolite**

5   Figure 4 shows the optimized configurations of 8T, 14T and 18T of the

6   extra-framework modified H₃PO₄/HZSM-5 zeolite. The detailed parameters and

7   deprotonation energy are listed in Table 3.

8

9   (a) 8T

10

11   (b) 14T

12

1   (c) 18T

2
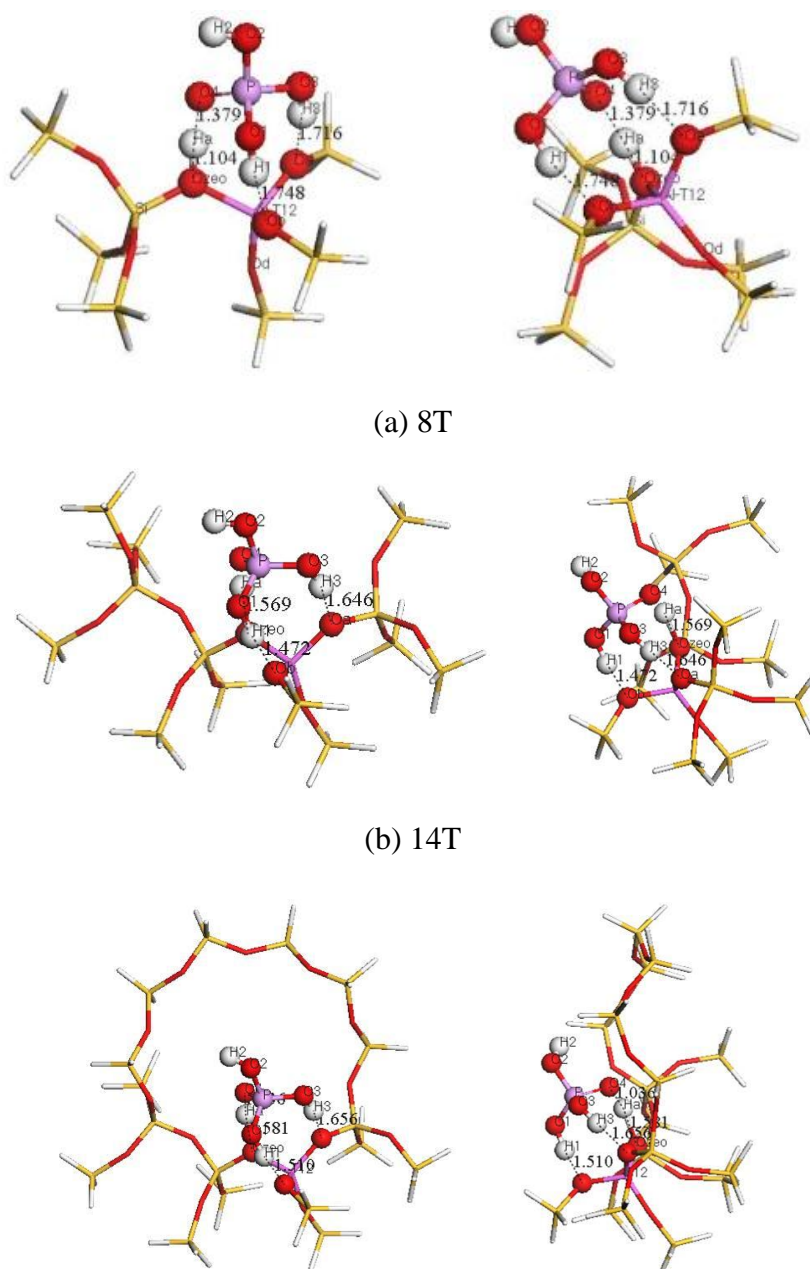
3   Figure 4 The optimized models of extra-framework modified ZSM-5 zeolite

4   Table 3 Deprotonation energy of the extra-framework modified ZSM-5 zeolite

Model	atoms	$E_{Zeo\text{-}OH}$ (Ha)	$E_{Zeo\text{-}O\text{-}}$ (Ha)	DPE (kcal/mol)
8T	42	-3452.0915	-3451.6159	298.41
14T	66	-5648.3875	-5647.9095	300.00
18T	81	-7186.7492	-7186.2677	302.17

5

6   From Figure 4 and Table 3, the H_1 and H_2 in phosphorus acid molecule form

7   hydrogen bonds with O atoms in zeolite, respectively. The O_4 atom in phosphorus

8   acid molecule forms hydrogen bond with the bridge hydroxyl in zeolite. The

9   deprotonation energy of each model is 298.41kcal/mol, 300.00kcal/mol and

10   302.17kcal/mol, respectively. The deprotonation energies of 14T and 18T are very

11   close.

12   Figure 5 shows the stable configurations of ethanol adsorbed on 8T, 14T and 18T

13   of extra-framework modified H_3PO_4/HZSM-5 zeolite. Table 4 lists the geometric

14   parameters and adsorption energy data of ethanol adsorbed on each model.
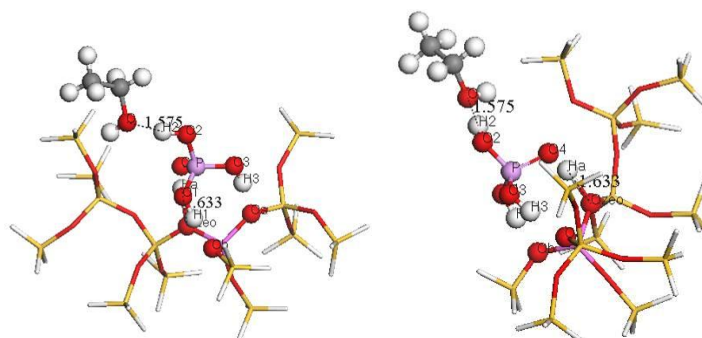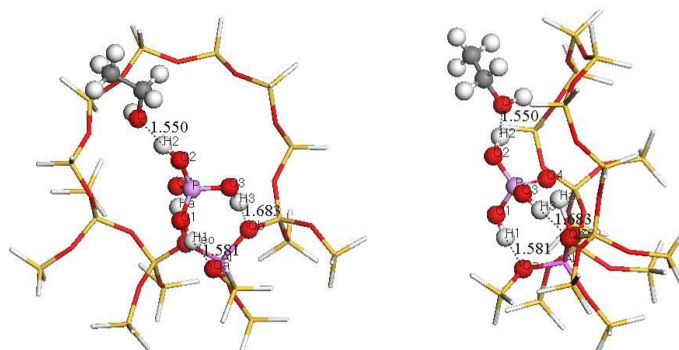
1

2 (a) 8T

3
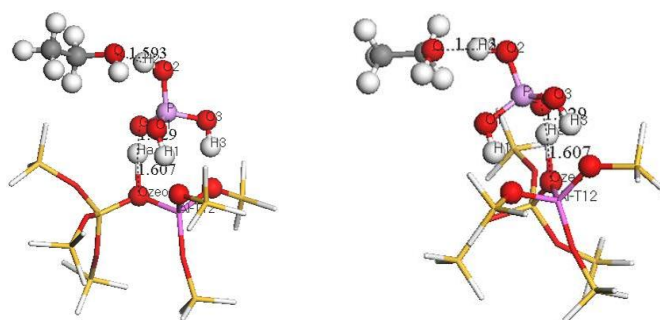
4 (b) 14T

5

6 (c) 18T

7 Figure 5 The configurations of ethanol adsorbed on the extra-framework modified

8 ZSM-5zeolite

9 Table 4 Adsorption energy of ethanol adsorbed on the extra-framework modified

10 ZSM-5 zeolite

Model	O_{zeo}-H_a (Å)	O-H_a (Å)	E_T (Ha)	E_{C2H5OH} (Ha)	$E_{T-C2H5OH}$ (Ha)	E_a (kcal/mol)

8T	1.027	1.593	-3452.0915	-155.0447	-3607.1607	-15.44
14T	1.633	1.575	-5648.3875	-155.0447	-5803.4548	-14.17
18T	1.638	1.550	-7186.7492	-155.0447	-7341.8187	-15.57

1   From Figure 5, in 8T, 14T and 18T, ethanol molecule forms hydrogen bond with

2   H_2 in phosphorus acid. But the configuration of 8T is different from that of 14T. From

3   Table 4, the distances between the O atom of ethanol molecule and H atom of the

4   bridge hydroxyl of zeolite are 1.593Å, 1.550Å and 1.603Å, respectively. The bond

5   lengths of bridge hydroxyl of zeolite are 1.027Å, 1.033Å and 1.021Å, respectively.

6   The difference of bond length between each other is within 0.1Å, suggesting the O

7   atom forms hydrogen bond with H atom of bridge hydroxyl of zeolite. The adsorption

8   energies of each model are -15.44kcal/mol, -14.17kcal/mol and -15.57kcal/mol,

9   respectively. The adsorption energy of 8T shows little difference from those of 14T

10   and 18T.

11   In summary, as for extra-framework modified H_3PO_4/HZSM-5 zeolite, the

12   configuration of 14T with ethanol absorbed is close to that of 18T. Thus, 8T is not

13   suitable to be used to study the related properties of extra-framework modified

14   H_3PO_4/HZSM-5 zeolite.

15   **3.1.3 Framework Modified H_3PO_4/HZSM-5 Zeolite**

16   Figure 6 shows the configurations of 8T, 14T and 18T of framework modified

17   H_3PO_4/HZSM-5 zeolite. The detailed parameters and deprotonation energy are listed

18   in the Table 5.

15

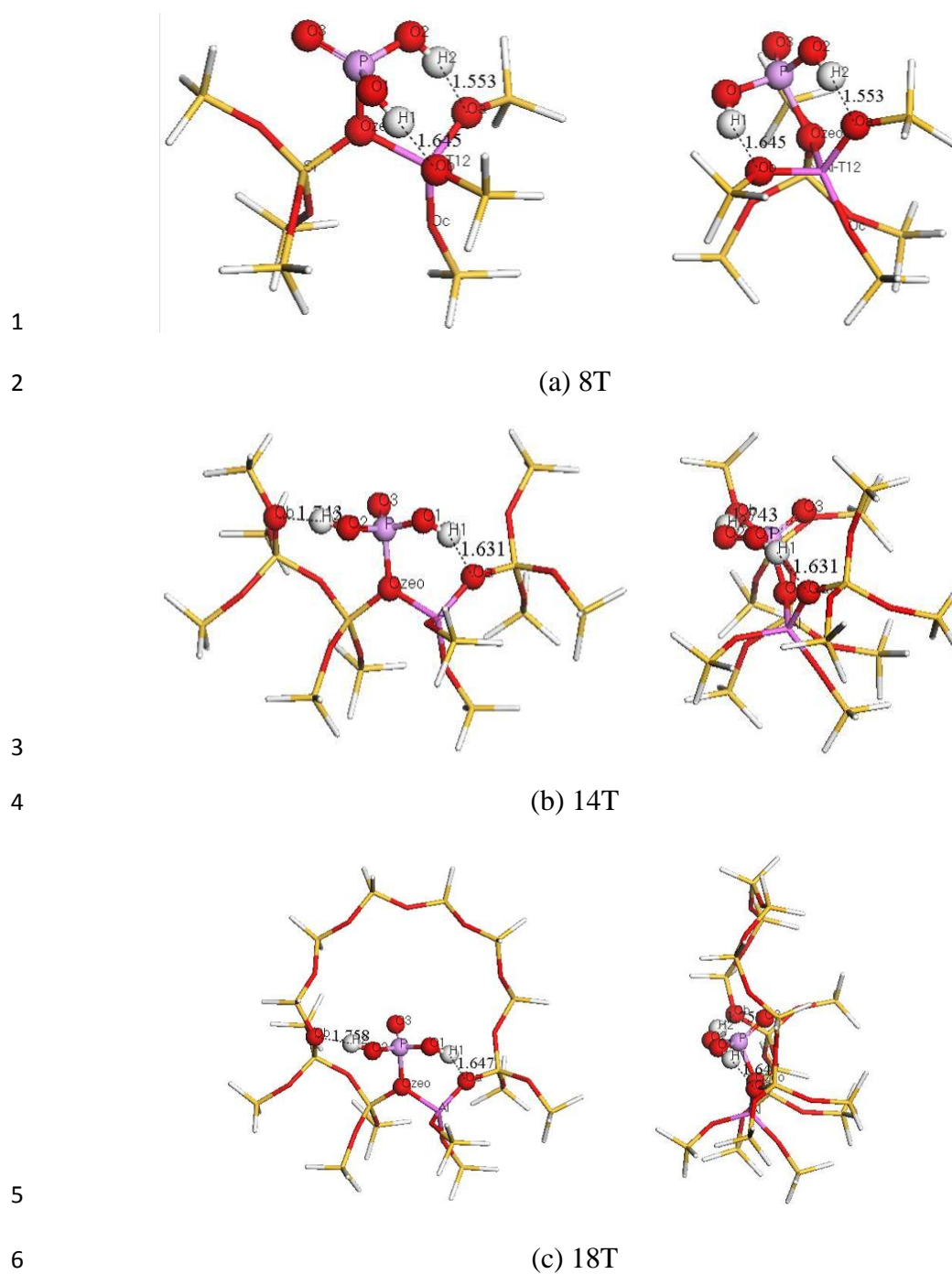(a) 8T

(b) 14T

(c) 18T

Figure 6 The configurations of P framework modified ZSM-5 zeolite

Table 5 Deprotonation energy of the P framework modified ZSM-5 zeolite

| Model	atoms	E_{Zeo-OH} (Ha)	E_{Zeo-O-} (Ha)	DPE (kcal/mol)
8T	39	-3375.5873	-3375.1027	304.13

16

14T	63	-5571.8819	-5571.3960	304.94
18T	78	-7110.2415	-7109.7543	305.76

1   From Figure 6, the optimized configuration of 8T is greatly different from those

2   of 14T and 18T. However, the optimized configuration of 14T and 18T are almost the

3   same. In 8T, all the H atoms of $H_2PO_4^-$ form hydrogen bond with the O atoms on one

4   side of Al atom in the zeolite. In the 14T and 18T, however, the H atoms of $H_2PO_4^-$

5   form hydrogen bond with the O atoms on both sides of Al atom in zeolite.

6   From Table 5, the deprotonation energies of 8T, 14T and 18T are 304.13kcal/mol,

7   304.94kcal/mol   and   305.76kcal/mol,   respectively.   The   deprotonation   energy

8   difference between each model is within 2kcal/mol. The deprotonation energies of

9   14T and 18T are very close, with the difference of 0.78kcal/mol.

10   Figure 7 shows the stable configurations of 8T, 14T and 18T of ethanol adsorbed

11   on the framework modified $H_3PO_4/HZSM-5$ zeolite. The parameters and adsorption

12   energy data of ethanol on each model are listed in Table 6.

13

14   (a) 8T

1

2   (b) 14T

3

4   (c) 18T
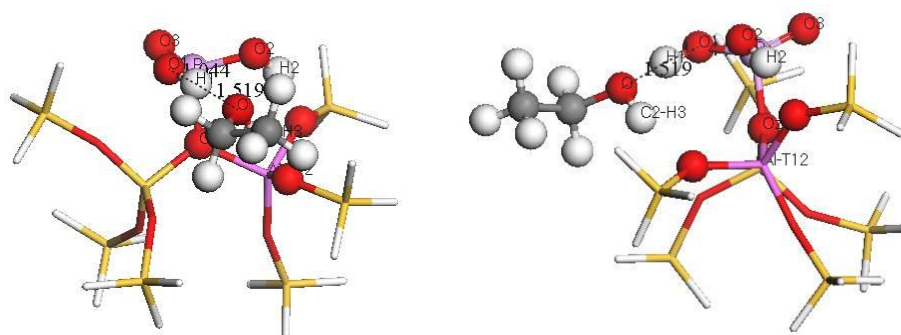
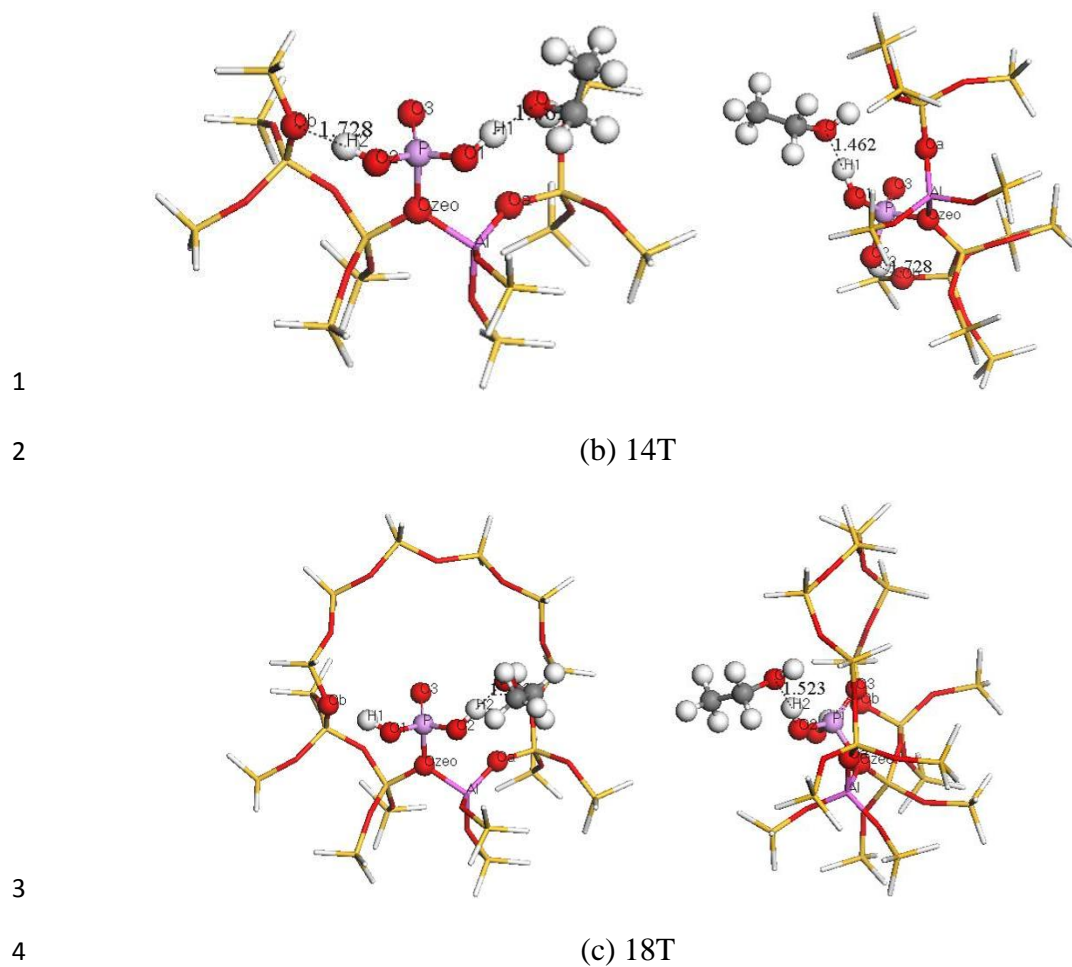5   Figure 7 The configurations of ethanol adsorbed on framework modified ZSM-5

6   zeolite

7   Table 6 Adsorption energy of ethanol adsorbed on framework modified ZSM-5 zeolite

Model	O_{zeo}-H_a (Å)	O-H_a (Å)	E_T (Ha)	E_{C2H5OH} (Ha)	$E_{T-C2H5OH}$ (Ha)	E_a (kcal/mol)
8T	1.044	1.519	-3375.5873	-155.0447	-3530.6532	-12.33
14T	1.051	1.462	-5571.8819	-155.0447	-5726.9359	-5.85
18T	1.039	1.523	-7110.2415	-155.0447	-7265.2981	-7.51

8   From Figure 7, whichever of 8T, 14T and 18T is chosen, ethanol molecule form

9   hydrogen bond with the H atom in phosphorus acid. However, because the 8T

18

1   configuration of framework modified H_3PO_4/HZSM-5 zeolite is greatly different from

2   those of 14T and 18T, leading to the result that the configuration of 8T is still greatly

3   different from those of 14T and 18T.

4   From Table 6, the distances between O atom of ethanol and H atom of bridge

5   hydroxyl in zeolite are 1.519Å, 1.462Å and 1.523Å, respectively. The bond lengths of

6   bridge hydroxyl in zeolite are 1.044Å, 1.051Å and 1.039Å, respectively. The

7   difference between the bond length data is within 0.1Å, suggesting O atom of ethanol

8   forms hydrogen bond with H atom of bridge hydroxyl in zeolite. The adsorption

9   energy of each model is -12.33kcal/mol, -5.85kcal/mol and -7.51kcal/mol,

10   respectively. The difference of adsorption energy of ethanol adsorbed on 14T and 18T

11   is within 2kcal/mol. The adsorption energy of 8T differs greatly from those of 14T

12   and 18T. The adsorption energy of 8T is almost double of that of 18T, suggesting the

13   adsorption energy of ethanol adsorbed on 8T differs greatly from those of 14T and

14   18T.

15   In summary, as for the parameters and deprotonation energy of the framework

16   modified H_3PO_4/HZSM-5 zeolite after optimization and with ethanol adsorbed, the

17   results of 8T differ greatly from those of 14T and 18T. However, the results of 14T

18   and 18T differ little. Therefore, 8T can't be used to study the related properties of the

19   framework modified H_3PO_4/HZSM-5 while both 14T and 18T can be used.

20   Through comparing the geometry configurations, deprotonation energy and

21   ethanol adsorption energy of 8T, 14T and 18T of ZSM-5 before and after P

22   modification, 14T was chosen as the computational model of the Transition State

19

1 search.

2 **3.2 Ethylene Adsorption**

3 In the framework modified H_3PO_4/HZSM-5 zeolite, two atoms of the phosphorus

4 acid form hydrogen bonds with O atoms of zeolite framework, which enhances the

5 stability of the configuration, but makes it more difficult for ethylene molecules to be

6 adsorbed on the acidic sites of the framework modified H_3PO_4/HZSM-5 zeolite. In the

7 extra-framework modified H_3PO_4/HZSM-5 zeolite, not only do two H atoms form

8 hydrogen bonds with O atoms of the zeolite framework, but also one H atom is

9 exposed in the channel of zeolite, which makes it easier for ethylene molecules to be

10 adsorbed on the extra-framework modified H_3PO_4/HZSM-5 zeolite. Thus, after

11 calculation, the properties of the extra-framework modified H_3PO_4/HZSM-5 zeolite

12 and unmodified HZSM-5 zeolite are compared.

13 Figure 8 shows the stable configurations of ethylene adsorbed on the catalyst

14 model before and after ZSM-5 modification. The distances between C_1 atom and C_2

15 atom of ethylene with acidic protons of the catalyst, H_a and H_2, are listed in Table 7.

16 From Figure 8 and Table 7, on the unmodified catalyst model, ethylene forms

17 hydrogen bond with the acidic proton of the catalyst while on the extra-framework

18 modified H_3PO_4/HZSM-5 zeolite, ethylene forms hydrogen bond with H_2 atom of

19 phosphorus acid in the catalyst model.

20

1

2   (a) Un- Front View   (b) Un- Side View

3

4   (c) Ex- Front View   (d) Ex-Side View
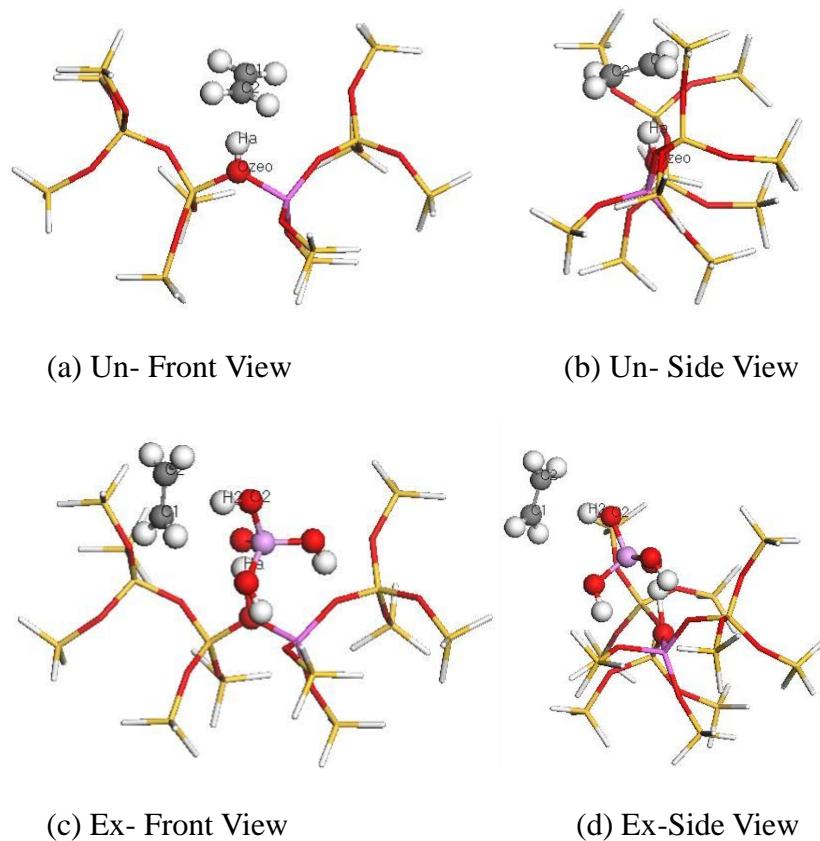
5   Figure 8 The configurations of ethylene adsorbed on the unmodified and modified

6   ZSM-5 zeolite

7 *Un-: unmodified ZSM-5 zeolite;

8 Ex-: extra-framework ZSM-5 zeolite;

9

10 Table 7 Geometric parameters of ethylene adsorbed on the unmodified and modified

11   ZSM-5 zeolite

Model	C-H (Å)				C-O (Å)			C-C (Å)
Un	C_1-H_a	2.270	C_2-H_a	2.261	C_1-O_{zeo} 3.234	C_2-O_{zeo} 3.214		1.343
Ex	C_1-H_2	2.318	C_2-H_2	2.348	C_1-O_2 3.298	C_2-O_2 3.272		1.342

12   The adsorption energy of ethylene on the unmodified and modified ZSM-5

1   zeolite is listed in Table 8. The value of adsorption energy of ethylene on the

2   unmodified ZSM-5 agrees with the values calculated by Wang[47]. From Table 8, on

3   the extra-framework modified H_3PO_4/HZSM-5 zeolite, the adsorption energy of

4   ethylene decreases, which makes the products desorb quickly after formation and

5   reduces the incidence of dimerization or polymerization.

6   Table 8 Adsorption energy of ethylene adsorbed on the unmodified and modified

7   ZSM-5 zeolite

Model	E_T (Ha)	E_{C2H4} (Ha)	E_{T-C2H4} (Ha)	E_a (kcal/mol)	E_a (kJ/mol)
Un	-5004.0379	-78.5759	-5082.6296	-9.88	-41.34
Ex	-5648.3875	-78.5759	-5726.9732	-6.10	-25.54

8   **3.3 Ethylene Protonation**

9   Figure 9 shows the stable configurations of ethyl on the unmodified and

10 modified ZSM-5 zeolite. To ensure that the atoms of reactants and products can

11 completely be matched when transition state search is conducted, adsorption

12 configuration of ethyl on the catalyst is obtained through moving the adsorption

13 configuration of ethylene. Table 10 lists the adsorption energy of ethyl on the catalyst.

14

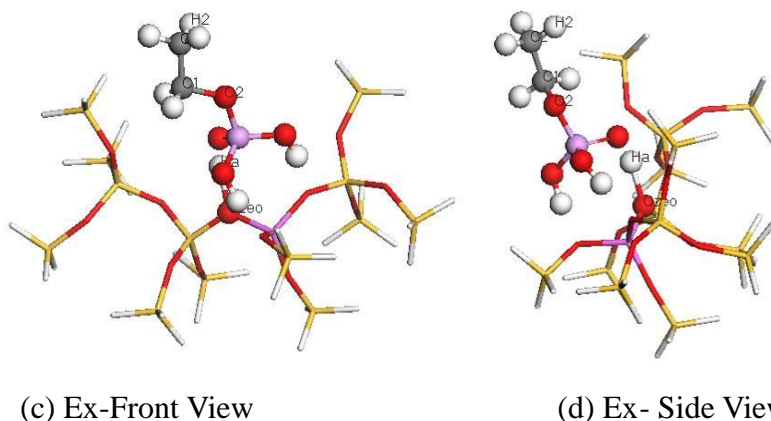15   (a) Un- Front View   (b) Un-Side View

1

2   (c) Ex-Front View   (d) Ex- Side View
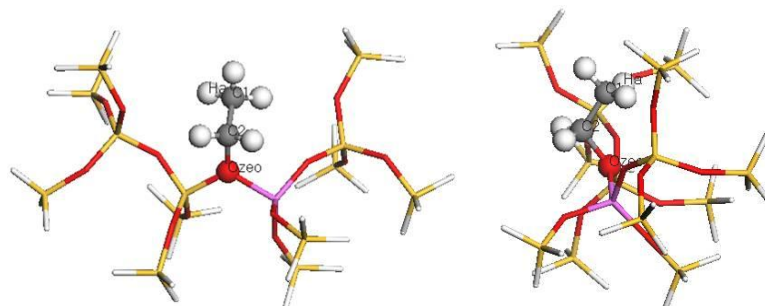
3   Figure 9 The configurations of C_2H_5 adsorbed on the unmodified and modified

4   ZSM-5 zeolite

5

6   Table 9 Geometric parameters of C_2H_5 adsorbed on the unmodified and modified

7   ZSM-5 zeolite

Model	C-H (Å)				C_1-O_2 (Å)	C-C (Å)
Un	C_1-H_a	2.270	C_2-H_a	2.261	1.534	1.514
Ex	C_1-H_2	2.318	C_2-H_2	2.348	1.495	1.517

8

9   Table 10 Adsorption energy of C_2H_5 adsorbed on the unmodified and modified

10   ZSM-5 zeolite

Model	E_T (Ha)	E_{C2H4} (Ha)	E_{T-C2H5} (Ha)	ΔE (kcal/mol)	ΔE (kJ/mol)
Un	-5004.0379	-78.5759	-5082.6385	-15.45	-64.65
Ex	-5648.3875	-78.5759	-5726.9863	-14.32	-59.92

3.4 The Transition State Search of Ethylene Protonation Reaction before and after Modification

The stable configurations of ethylene adsorption and ethylene protonation were investigated above. The transition state search was conducted with $Dmol^3$ module. Figure 10 shows the energy figures of the ethylene protonation reaction and the transition state configurations of the unmodified and modified ZSM-5 zeolite. Table 11 lists the geometric parameters of transition state configurations of ethylene protonation.

From Figure 10 and Table 11, on the unmodified ZSM-5 zeolite, H_a of bridge hydroxyl moves close to C_1, with the distance changing from 2.270Å to1.202Å. C_2 of ethanol moves close to O_{zeo} of the bridge hydroxyl of the zeolite, with the distance changing from 3.214Å to 2.493Å. The bond length of C-C in ethylene changes from 1.343Å to 1.398Å. Then, H_a atom moves closer to C_1, and C_2 moves closer to O_{zeo} until ethylene is protonated. On extra-framework modified H_3PO_4/HZSM-5 zeolite, H_2 of the phosphorus acid moves close to C_2 of ethylene, with the distance changing from 2.348Å to 1.216Å. The C_1 of ethylene moves close to O_2 of phosphorus acid, with the distance changing from 3.298Å to 2.376Å. The bond length of C-C of ethylene changes from 1.342Å to 1.401Å. Then, H_2 moves closer to C_2 and C_1 moves closer to O_2 until the ethylene is protonated.
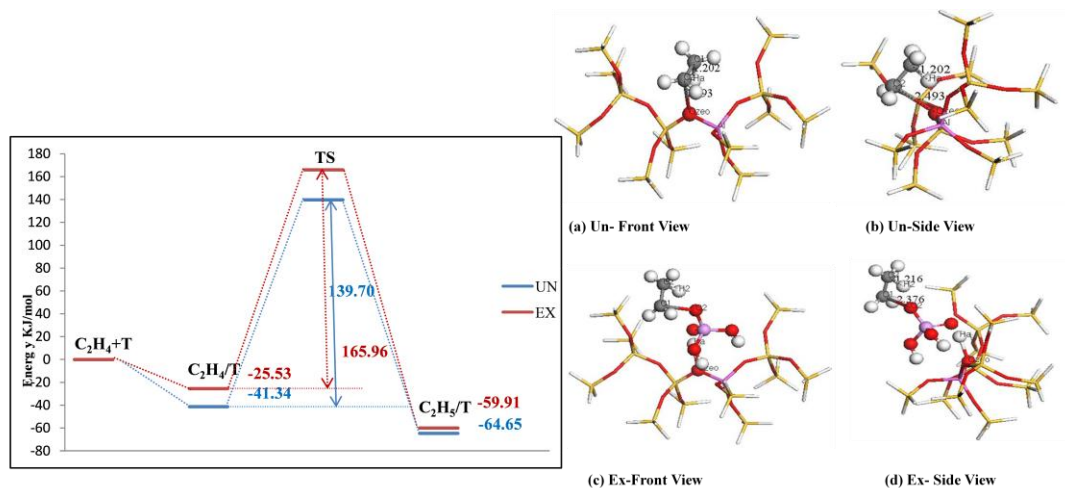
1

2   Figure 10 The energy figures of the ethylene protonation reaction

3   (a) and (b) are the transition state configuration of the ethylene protonation before modification

4   (c) and (d) are the transition state configuration of the ethylene protonation reaction after

5   modification

6   Table 11 Geometric parameters of the transition state of the ethylene

7   protonation reaction

Model	C-H (Å)		C-O (Å)		C-C (Å)
Un	C_1-H_a	1.202	C_1-O_{zeo}	2.493	1.398
Ex	C_2-H_2	1.216	C_2-O_2	2.376	1.401

8   The charge population analysis of ethylene protonation is shown in Table 12.

9   From Table 12, on the unmodified zeolite, O_{zeo} and C_1 obtain electrons while H_a and

10   C_2 lose electrons. The charge of H_a decreases from original +0.359|e| to +0.263|e| of

11   the Transition State (TS), suggesting Ha obtains electrons during the process of

12   reactant to the transition state. The charge of C_2 increases from original -0.200|e| to

13   +0.051|e|, suggesting C_2 loses electrons during the process of reactant to the transition

1   state. Therefore, during the process from reactants to the transition state, only C_2 loses

2   electrons. From Table 12, during the process from the transition state to products, only

3   C_2 loses electrons. All the results suggest that the C of ethylene that forms ethyl with

4   zeolite loses electrons. C-O bond between ethylene and zeolite is formed through

5   charge transfer.

6   Table 12 Mulliken population analysis of the ethylene protonation reaction

Model		Mulliken Charge |e|			
		C_1	C_2	$H_a(H_2)$	$O_{zeo}(O_2)$
Un	Reactant	-0.205	-0.200	0.359	-0.769
	TS	-0.253	0.051	0.263	-0.924
	Product	-0.228	0.100	0.093	-0.827
Ex	Reactant	-0.192	-0.176	0.305	-0.553
	TS	0.051	-0.237	0.267	-0.749
	Product	0.070	-0.207	0.097	-0.597

7

8   Figure 10 shows the energy change during the reaction process. C_2H_4+T

9   represents ethylene molecule and zeolite. C_2H_4/T represents ethylene adsorbed on

10   zeolite. TS represents the transition state. C_2H_5/T represents ethyl and zeolite.

11   From Figure 10, the reaction: C_2H_4+H-ZSM-5→C_2H_5-ZSM-5 can be obtained.

12   On the unmodified catalyst, the reaction activation energy is 139.70kJ/mol. On the P

13   modified catalyst, the reaction activation energy is 165.96kJ/mol. On the P modified

14   catalyst, the activation energy of ethylene protonation increases. That ethylene

26

1   protonation reaction is the rate-limiting step of ethylene dimerization suggests that

2   after P modification, the activation energy of ethylene dimerization increases to

3   inhibit ethylene dimerization, prevent deep ethylene polymerization and thus improve

4   the resistance to coke deposition of ZSM-5 and prolong the life of zeolite.

5   **4. Conclusions**

6   In this work, Density Functional Theory (DFT) was used to calculate the

7   activation energy of the rate-limiting step of ethylene dimerization, ethylene

8   deprotonation, on the unmodified and P-modified ZSM-5 zeolite. The following

9   conclusions can be obtained.

10   (1) 14T was used to search the transition state, after comparing the geometric

11   parameters, deprotonation energy and ethanol adsorption energy of 8T, 14T and

12   18T.

13   (2) On the extra-framework modified H_3PO_4/HZSM-5 zeolite, the adsorption energy

14   of ethylene decreases, which makes the products desorb quickly after formation

15   and reduces the incidence of dimerization or polymerization.

16   (3) Ethylene polymerization reaction is the main cause of coking deactivation of

17   ZSM-5. That ethylene protonation reaction is the rate-limiting step of ethylene

18   dimerization suggests that after P modification, the activation energy of ethylene

19   dimerization increases to inhibit ethylene dimerization, prevent deep ethylene

20   polymerization and thus improve the resistance to coke deposition of ZSM-5 and

21   prolong the life of zeolite.

22   **References**

1 [1] M. H. Zhang and Y. Z. Yu. Dehydration of Ethanol to Ethylene. Ind. Eng. Chem.

2 Res., 2013, 52 (28): 9505-9514.

3 [2] J. Sheehan. The Road to Bioethanol: A Strategic Perspective of the U.S.

4 Department of Energy's National Ethanol Program. NW Washington. Am. Chem. Soc.,

5 1997, 2-25.

6 [3] S. Bastianoni and N. Marchettini. Ethanol Production from Biomass: Analysis of

7 Process Efficiency and Sustainability. Biomass Bioenergy, 1996, 11(5): 411-418.

8 [4] G. W. Huber, S. Iborra and A. Corma. Synthesis of Transportation Fuels from

9 Biomass: Chemistry, Catalysts, and Engineering. Chem. Rev., 2006, 106(9):

10 4044-4098.

11 [5] C. B. Phillips and R. Datte. Production of ethylene from hydrous ethanol on

12 H-ZSM-5 under mild conditions. Ind. Eng. Chem. Res., 1997, 36(11): 4456-4475.

13 [6] E. Wang, J. X. Chen, and J. L. Li. New properties of SAPO-34 catalyst of ethanol

14 dehydration to ethylene . Guangxi Chem. Ind., 1991, 4: 1-3.

15 [7] L. J. gong, C. Han, and T. W. Tan. Research on preparation of bio-ethylene. Mod.

16 Chem. Ind., 2006, 26(4): 44-47.

17 [8] T. Isao, S. Masahiro, and I. Megumu. Dehydration of ethanol into ethylene over

18 solid acid catalysts. Catal. Lett., 2005, 105(3-4): 249-252.

19 [9] G. Yesim, and D. Timur. Ethylene and acetaldehyde production by selective

20 oxidation of ethanol using mesoporous V-MCM-41 catalysts. Ind. Eng. Chem. Res.,

21 2006, 45(10): 3496-3502.

22 [10] S. A. Barthos, and F. Solymosi. Decomposition and aromatization of ethanol on

1   ZSM-5 based catalysts. J. Phys. Chem., 2006, 110(43): 21816-21825.

2   [11] R. L. V. Mao. Catalytic conversion of aqueous ethanol to ethylene. US patent,

3   4873392, 1989-12-24.

4   [12] R. L. V. Mao, and L. H. Dao. Ethylene Light Olefins from Ethanol. US patent,

5   4698452, 1987-10-06.

6   [13] S. Bun, S. Nishiyama, and S. Tsuruya. Ethanol Conversion over Ion-Exchanged

7   ZSM-5 Zeolites. Appl. Catal., 1990, 59(1): 13-29.

8   [14] I. Takahara, M. Saito, and M. Inaba. Dehydration of Ethanol into Ethylene over

9   Solid Acid Catalysts. Catal. Lett., 2005, 105(3-4): 249-252.

10   [15] J. Ouyang, F. X. Kong, and G. D. Su. Catalytic Conversion of Bio-ethanol to

11   Ethylene over La-Modified HZSM-5 Catalysts in a Bioreactor. Catal. Lett., 2009,

12   132(1-2): 64-74.

13   [16] K. Murata, M. Inaba, and I. Takahara. Effects of surface modification of

14   H-ZSM-5 catalysts on direct transformation of ethanol into lower olefins. J. Jpn.

15   Petrol. Inst., 2008, 51(4):234-239.

16   [17] D. S. Zhang, R. J. Wang, and X. X. Yang. Effect of P content on the catalytic

17   performance of P-modified HZSM-5 catalysts in dehydration of ethanol to ethylene.

18   Catal. Lett., 2008, 124(3-4):384-391.

19   [18] K. Ramesh, L. M. Hui, and Y. F. Han. Structure and reactivity of phosphorous

20   modified H-ZSM-5 catalysts for ethanol dehydration. Catal. Commun., 2009,

21   10(5):567-571.

22   [19] Q. T. Sheng, S. Q. Guo. Catalytic Dehydration of Ethanol to Ethylene over

Alkali-Treated HZSM-5 Zeolites. J. Brazil. Chem. Soc., 2014, 25(8): 1365-1371.

[20] J. Schulz, F. Bandermann. Conversion of ethanol over zeolite H-ZSM-5. Chem. Eng. Technol., 1994, 17(3): 179–186.

[21] Y. Chu, B. Han, A. M. Zheng, F. Deng. Influence of Acid Strength and Confinement Effect on the Ethylene Dimerization Reaction over Solid Acid Catalysts: A Theoretical Calculation Study. J. Phys. Chem. C, 2012, 116(23): 12687-12695.

[22] H. Yamazaki, T. Yokoi. Ethene oligomerization on H-ZSM-5 in relation to ethoxy species. Catal. Sci. Technol.,2014, Advance Article.

[23] J. H. Li, D. H. Zhou, J. Ren. Theoretical Study of Ethylene Dimerization on the Ga/HZSM-5 Zeolite. Acta. Phys. Chim. Sin., 2011, 27(6),1393-1399.

[24] J. Meeprasert, S. Choomwattana, P. Pantu and J. Limtrakul. Dehydration of Ethanol into Ethylene over H-MOR: A Quantum Chemical Investigation of Possible Reaction Mechanisms in the Presence of Water. NSTI NANOTECH, 2009, 3:288-291.

[25] N. Hansen, T. Bruggemann, A. T. Bell, and F. J. Keil. Theoretical Investigation of Benzene Alkylation with Ethene over H-ZSM-5. J. Phys. Chem. C 2008, 112(39), 15402–15411.

[26] J. Zhang, D. H. Zhou, and D. Ni. Investigation on ethylene dimerization over H-ZSM-5 zeolite by theoretical calculation. Chin. J. Catal., 2008, 29: 715-719.

[27]A. Chatterjee, and R. Vetrivel. Computer simulation studies on the role of templating organic molecules in the synthesis of ZSM-5. J. Chem. Soc., Faraday Trans., 1995, 91: 4313-4319.

[28] A. Chatterjee, and R. Vetrivel. Simulation studies on the role of templating organic molecules in the synthesis of microporous materials: 2. Modelling the electronic interaction between the templating molecules and ZSM-5. J. Mol. Catal. A: Chem., 1996, 106:75-81.

[29] A. Redondo, and P. J. Hay. Quantum Chemical Studies of Acid Sites in Zeolite ZSM-5. J. Phys. Chem., 1993, 97:11754-11761.

[30] A. Chatterjee, and A.K. Chandra. Fe and B substitution in ZSM-5 zeolites: a quantum-mechanical study. J. Mol. Catal. A: Chem., 1997, 119:51-56.

[31] M.S. Stave, and J.B. Nicholas. Density Functional Studies of Zeolites. 2. Structure and Acidity of [T]-ZSM-5. J. Phys. Chem., 1995, 99:15046-15061.

[32] J.G. Fripiat, F. Berger-André, J.-M. André, and E.G. Derouanc. Non-empirical quantum mechanical calculations on pentasil-type zeolites. Zeolites, 1983, 3(4):306-310.

[33] E.G. Derouane, and J.G. Fripiat. Non-empirical quantum chemical study of the siting and pairing of aluminium in the MFI framework. Zeolites, 1985, 5:165-172.

[34] S.R. Lonsinger, A.K. Chakraborty, D.N. Theodorou, and A.T. Bell. The Effects of Local Structural Relaxation on Aluminum Siting Within H-ZSM-5. Catal. Lett., 1991, 11:209-217.

[35] A. Chatterjee, and R. Vetrivel. Electronic and structural properties of aluminum in the ZSM-5 framework. Microporous Mater., 1994, 3:211-218.

[36] Y. P. Huang, X. Q. Dong, M.M Li, M. H. Zhang and Y. Z. Yu. Density Functional

Theory Study on Structural and Electronic Properties of H3PO4/ZSM-5. RSC Adv., 2014, 4 (28), 14573 - 14581.

[37] B. Delley. An All-Electron Numerical Method for Solving the Local Density Functional for Polyatomic Molecules. J. Chem. Phys., 1990, 92:508-517.

[38] B. Delley. From molecules to solids with the DMol3 approach. J. Chem. Phys., 2000, 113:7756-7764.

[39] M. Elanany, M. Koyama, M. Kubo, P. Selvam and A. Miyamoto. Periodic density functional investigation of Bronsted acidity in isomorphously substituted chabazite and AlPO-34 molecular sieves. Microporous Mesoporous Mater., 2004, 71:51-56.

[40] B. Kalita and R. C. Deka. DFT study of CO adsorption on neutral and charged Pdn(n =1–7) clusters. Eur. Phys. J. D., 2009, 53:51-58.

[41] Y. Wang, G. Yang, D. H. Zhou, X. H. Bao. Density functional theory study of chemical composition influence on the acidity of H-MCM-22 zeolite. J. Phys. Chem. B, 2004, 108(47):18228-18233.

[42] H. C. Xin, X. P. Li, Y. Fang, X. F. Yi, W. H. Hu, Y. Y. Chu, F. Zhang, A. M. Zheng, H. P. Zhang, X. B. Li. Catalytic dehydration of ethanol over post-treated ZSM-5 zeolites. J. Catal., 2014, 312(0): 204-215.

[43] H. J. Fang, A. M. Zheng, S. H. Li, J. Xu, L. Chen, F. Deng. New Insights into the Effects of Acid Strength on the Solid Acid-Catalyzed Reaction: Theoretical Calculation Study of Olefinic Hydrocarbon Protonation Reaction. J. Phys. Chem. C, 2010, 114, 10254–10264.

1   [44] M. Brandle, J. Sauer. Acidity differences between inorganic solids induced by

2   their framework structure. A combined quantum mechanics molecular mechanics ab

3   initio study on zeolites. JACS, 1998, 120(7): 1556-1570.

4   [45] A. M. Zheng, L. Chen, J. Yang, M. J. Zhang, Y. C. Su, Y. Yue, C. H. Ye, F.

5   Deng. Combined DFT Theoretical Calculation and Solid-State NMR Studies of Al

6   Substitution and Acid Sites in Zeolite MCM-22: J. Phys. Chem. B, 2005,

7   109(51):24273–24279.

8   [46] C. C. Lee, R. J. Gorte, W. E. Farneth. Calorimetric Study of Alcohol and Nitrile

9   Adsorption Complexes in H-ZSM-5. J. Phys. Chem. B, 1997,101(19), 3811−3817.

10 [47] S. P. Wang, Y. L. Wang. Theoretical Study on the Acidity of Neighboring Acid

11 Sites in ZSM-5 Zeolite and Its Effect on Ethylene Protonation. Chin. J. Catal., 2009,

12 30(4): 305-311.